

Analytical Calculation of Intracellular Calcium Wave Characteristics

Raz Kupferman,* Partha P. Mitra,* P. C. Hohenberg,# and Samuel S.-H. Wang[§]

*Bell Laboratories, Lucent Technologies, Murray Hill, New Jersey 07974; #Department of Physics, Yale University, New Haven, Connecticut 06520-8120; and [§]Department of Neurobiology, Duke University Medical Center, Durham, North Carolina 27710 USA

ABSTRACT We present a theoretical analysis of intracellular calcium waves propagated by calcium feedback at the inositol 1,4,5-trisphosphate (IP₃) receptor. The model includes essential features of calcium excitability, but is still analytically tractable. Formulas are derived for the wave speed, amplitude, and width. The calculations take into account cytoplasmic Ca buffering, the punctate nature of the Ca release channels, channel inactivation, and Ca pumping. For relatively fast buffers, the wave speed is well approximated by $V_{\infty} = (J_{\text{eff}}D_{\text{eff}}/C_0)^{1/2}$, where J_{eff} is an effective, buffered source strength; D_{eff} is the effective, buffered diffusion constant of Ca; and C_0 is the Ca threshold for channel activation. It is found that the saturability and finite on-rate of buffers must be taken into account to accurately derive the wave speed and front width. The time scale governing Ca wave propagation is T_r , the time for Ca release to reach threshold to activate further release. Because IP₃ receptor inactivation is slow on this time scale, channel inactivation does not affect the wave speed. However, inactivation competes with Ca removal to limit wave height and front length, and for biological parameter ranges, it is inactivation that determines these parameters. Channel discreteness introduces only small corrections to wave speed relative to a model in which Ca is released uniformly from the surface of the stores. These calculations successfully predict experimental results from basic channel and cell parameters and explain the slowing of waves by exogenous buffers.

INTRODUCTION

Planar waves, spiral waves, and oscillations are observed in a large variety of biological systems (reviewed by Winfree, 1987). These spatiotemporally complex phenomena are manifestations of the excitable nature of individual cells or aggregates of cells. One widespread example in eukaryotes is the initiation and propagation of calcium waves in eggs and other cells (Berridge, 1993). Calcium waves are triggered by the activation of receptors on the cell surface. This stimulates the production of inositol-1,4,5-trisphosphate (IP₃), which diffuses through the cytosol and activates internal IP₃-sensitive receptors (IP₃R) that open and allow Ca²⁺ to be released from an intracellular store, the endoplasmic reticulum (ER). The wave is then propagated across the cell by positive feedback of released cytosolic Ca²⁺ that further activates the IP₃R (Finch et al., 1991; Iino and Endo, 1992; Lechleiter et al., 1991; Wang and Thompson, 1995).

Theoretical investigations of these intracellular calcium waves have been carried out using continuum reaction-diffusion models (DeYoung and Keizer, 1992; Sneyd et al., 1993; Atri et al., 1993; Tang and Othmer, 1994; Wagner and Keizer, 1994; Jafri and Keizer, 1995). Most studies so far have attempted to construct models that are as realistic as possible by fitting the functional structure of the various building blocks (e.g., channel characteristics, Ca²⁺ pumps, and buffer kinetics) to experimental data.

Given the particular parameters of a biological system, numerical simulation can yield an exact solution, and these models give planar, circular, and spiral waves that reproduce experimental observations. However, when the details of the phenomenon are not understood precisely, this can be an overly restrictive approach. Furthermore, exploration of a multidimensional parameter space by numerical methods is impractical.

Analytical methods, on the other hand, produce formulas that can lead to more physical insights into a problem. Such insights begin with the identification of appropriate groupings of parameters that capture the natural scales of the phenomenon. Analytical formulas thus obviate the need for exploration of parameter space. Finally, once calculations are in hand, they are more easily generalized to accommodate new, unforeseen features of the system.

Here we construct a model that is analytically tractable, in part by discarding some of the fine details found in the more extended models. We are able then to derive simple formulas for the velocity and wavefront length for planar waves. Our main goal is to identify the factors that play a central role in determining the main wave characteristics. We concentrate on the case in which IP₃ is uniformly elevated in the cell and the waves are limited by calcium diffusion.

As our starting point, we used a model analogous to the FitzHugh-Nagumo model, originally used to describe nerve impulse conduction (for a review see Murray, 1989). Following McKean (1970) and Rinzel and Keller (1973), we expressed the feedback properties as step functions, in this case the activation and inactivation properties of the IP₃ receptor as functions of Ca²⁺. This approximation allows an analytical solution for wavefront and pulse propagation.

Our work additionally takes into account three previously neglected aspects of calcium excitability. The first is the fact

Received for publication 29 February 1996 and in final form 19 February 1997.

Address reprint requests to Dr. Raz Kupferman, Lawrence Berkeley National Laboratory, 50A-2152, 1 Cyclotron Road, Berkeley, CA 94720. E-mail: raz@csr.lbl.gov.

© 1997 by the Biophysical Society

0006-3495/97/06/2430/15 \$2.00

that Ca^{2+} reacts with endogenous and exogenous buffers at finite rates. Earlier studies that considered the presence of buffers either subsumed their effect in an effective diffusion constant or assumed very fast reaction rates (Wagner and Keizer, 1994; Sneyd et al., 1995; Jafri and Keizer, 1995). These assumptions overlook the possibility that calcium emanating from a channel may be able to stimulate further calcium release before it has come into binding equilibrium with buffers—a competition between the time scales of buffering and channel activation. Experiments with added exogenous buffers suggest that buffer kinetics do indeed play an important role in determining the characteristics of Ca^{2+} waves (Wang and Thompson, 1995), and among our goals is establishing a theoretical understanding of these recent measurements.

A second aspect of calcium excitability previously disregarded is the punctate nature, or discreteness of the calcium channels (see, however, Dupont and Goldbeter, 1994). For a continuum approach to be justified, the spacing between channels must be shorter than all other length scales associated with the phenomenon, including those that are not apparent as experimentally measured parameters but are still intrinsic to the mechanism. This is in fact not the case, but it will be shown that the required corrections induced by channel discreteness are small for the parameter ranges considered here.

Third and finally, we clarify the effect of inactivation on pulse width and height. We find that in biological ranges of parameter values, Ca^{2+} release in a passing wave is terminated by channel inactivation. This sets peak Ca^{2+} concentration and front length, but not the wave speed, which is only minimally affected by inactivation.

The main results of this paper may be summarized as follows. The dimensional combination of parameters that gives the scale of the propagation speed of calcium waves is $(J_{\text{eff}}D_{\text{eff}}/C_0)^{1/2}$, where J_{eff} is the effective free Ca^{2+} influx when the channels are activated, D_{eff} is the effective diffusion constant of calcium, and C_0 is a concentration scale that corresponds to the channel activation threshold. This combination has the form $(D_{\text{eff}}/T_r)^{1/2}$, where $T_r = C_0/J_{\text{eff}}$ reflects the time needed for calcium release to activate further release (cf. Luther's equation; Luther, 1906; Jaffe, 1991).

The propagation speed is strongly dependent on buffer concentration and buffer kinetics. The presence of fast buffers significantly slows down the wave, whereas the presence of slow buffers does not. The fast buffer kinetics regime applies for $K_f B \gg J_0/C_0$, where K_f is the Ca^{2+} buffer forward reaction rate, $B = [\text{B}]_{\text{total}}$ is the total concentration of buffer sites, and J_0 is the *total*, unbuffered ("bare") calcium flux through activated channels. Under this condition, the propagation speed of a planar wave is approximately given by

$$V \approx \left(\frac{J_{\text{eff}} D_{\text{eff}}}{C_0} \right)^{1/2} \left(1 + \frac{J_0}{2C_0 K_f B} \right) \quad (1)$$

where

$$J_{\text{eff}} = \frac{J_0}{\bar{\kappa}} \quad \text{and} \quad D_{\text{eff}} = \frac{D + D_b(\bar{\kappa} - 1)}{\bar{\kappa}} \quad (2)$$

where D is the diffusion constant of free Ca^{2+} , and D_b is that of the buffers and buffer-bound Ca^{2+} , which we assumed to be equal. The dimensionless quantity $\bar{\kappa}$ is an averaged buffer capacity. In the opposite regime of slow buffer kinetics, the scale of the wave speed is determined entirely by the bare parameters for free Ca^{2+} :

$$V \approx \left(\frac{J_0 D}{C_0} \right)^{1/2} \left(1 - \frac{3C_0}{2J_0} K_f B \right) \quad (3)$$

Relative to a continuum model, wave speed is reduced when the Ca^{2+} source is composed of physically discrete channels. The magnitude of this effect depends on the dimensionless channel spacing, a , which in turn is a function of the actual channel spacing, A . For fast buffers, $a = A(J_{\text{eff}}/C_0 D_{\text{eff}})^{1/2}$, and for slow buffers $a = A(J_0/C_0 D)^{1/2}$. The wave speed is slower than the prediction of a continuum source model by a factor of $1 - O(a^{3/2})$. However, for physiological parameters this effect reduces the speed by only a few percent.

Because they are slow on the timescale T_r , channel inactivation and pumping activity have only small effects on the wave speed. However, the channel inactivation time, T_{in} , does determine the wave amplitude, C_{max} , and the width of the rising front, W , which are given by

$$C_{\text{max}} \approx J_{\text{eff}} T_{\text{in}} \quad \text{and} \quad W \approx V T_{\text{in}} \quad (4)$$

THE MECHANISM OF Ca^{2+} EXCITABILITY

Calcium waves start from a resting state in which the concentration of intracellular Ca^{2+} is four orders of magnitude lower than in the extracellular medium. Calcium release is triggered when an external agonist binds to a cell-surface receptor. This reaction stimulates, through a G-protein, the production of IP_3 , a water-soluble carbohydrate. IP_3 diffuses then through the cytosol, and binds to receptors embedded in the surface of the ER. The receptor protein is an IP_3 -gated channel that allows the release of Ca^{2+} from the ER into the cytoplasm.

IP_3 R channel opening not only requires IP_3 , but also depends on local Ca^{2+} concentration (Bezprozvanny et al., 1991; Finch et al., 1991; Iino and Endo, 1992). Although the exact mechanism of IP_3 R gating is not known in detail, the functional states of the IP_3 R can be described as closed, open (conducting), and inactivated. The channel is closed when the ambient calcium concentration is low, and the probability of being open increases when the Ca^{2+} concentration exceeds a certain activation threshold. Activated channels can then go into an inactivated state. Like activation, inactivation rates are faster at higher Ca^{2+} levels. However, inactivation takes place on a longer time scale than activation. These strongly nonlinear properties of the

IP₃R constitute a feedback mechanism—positive in the case of activation, and negative for inactivation.

Another calcium release channel with similar calcium feedback properties is the ryanodine receptor (Gyorke and Fill, 1993). Unlike IP₃R, these channels only require calcium to open. Our model considers only calcium feedback, and therefore (with appropriate parameter replacement) can be applied as well to systems in which ryanodine receptors provide direct calcium-induced calcium release, without the formation of IP₃.

After the passage of a calcium wave, the low Ca²⁺ concentration is restored by means of ion pumps and antiporters. Pumps are found both on the plasma membrane and on the surface of the ER. These pumps and antiporters have heterogeneous properties, but even for fairly large deflections from the resting Ca²⁺ level, the relaxation due to pumping activity has been observed to fall with a single exponential decay rate (Tse et al., 1994; but see also Herrington et al., 1996).

Calcium is also strongly buffered in the cell. Measurements in cells indicate that buffer-bound calcium is at least an order of magnitude less mobile than free Ca²⁺ (Baker and Crawford, 1972; Neher and Augustine, 1992; Allbritton et al., 1992); thus the apparent molecular weight of the buffers is 10⁶ or higher. The identity of these buffers is for the most part unknown, but they include proteins such as parvalbumin and calbindin.

These pumping and buffering mechanisms work against a continual leak of calcium from the internal calcium stores and from the extracellular fluid. The steady resting state thus attained has a free Ca²⁺ level in the range of 10–100 nM.

ANALYSIS OF SIMPLE MODELS OF CALCIUM WAVE PROPAGATION

In this section we present calculations that identify the features of calcium wave systems essential to adequately characterizing calcium excitability. We achieve this by first constructing a minimal model that incorporates positive feedback of Ca²⁺ on the IP₃ receptor and calcium pumping. We then consider how the results are affected by Ca²⁺ buffering, channel discreteness, and channel inactivation.

The minimal model: a continuously distributed Ca²⁺ source without inactivation or buffers

We consider the propagation of planar waves along the \tilde{X} axis (Fig. 1). We make the following assumptions: 1) The Ca²⁺ source is continuously and uniformly distributed throughout the cell volume. 2) The IP₃ receptor has two states. The channels are closed if the local Ca²⁺ concentration is below a critical threshold, C_0 , and are activated instantaneously when the concentration exceeds C_0 . The rate of calcium release when the channels are activated is J_0 . 3) Ca²⁺ is pumped out from the cytosol at a rate proportional to the concentration, with rate constant Γ . 4) Buffers

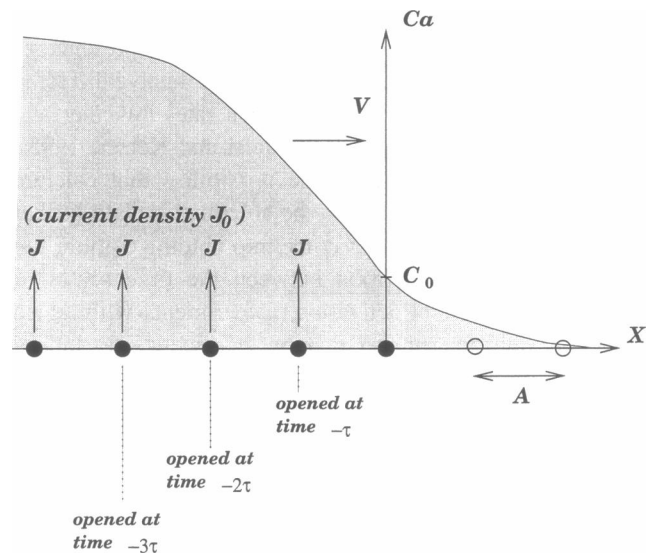


FIGURE 1 Calcium wavefront propagation. The minimum model assumes Ca²⁺ sources that are continuously and uniformly distributed with source strength per unit length J_0 . Channels are closed at rest (O), and are activated (●) when the local Ca²⁺ concentration rises above the activation threshold C_0 ($c = 1$ in dimensionless units). The wave propagates in the positive x direction at speed V . In the discrete model, the continuous calcium source is replaced by channels of strength J , uniformly spaced at intervals A (a in dimensionless units). Channels open successively at time intervals $\tau = A/V$.

and channel inactivation are ignored. 5) IP₃ is elevated to a level that allows wave propagation.

Under these assumptions, the evolution of the Ca²⁺ concentration field, $C(\tilde{X}, T)$, is governed by the differential equation

$$\frac{\partial C}{\partial T} = D \frac{\partial^2 C}{\partial \tilde{X}^2} - \Gamma C + J_0 \Theta(C - C_0) \quad (5)$$

where D is the diffusion constant of Ca²⁺ in the cytosol, and $\Theta(C - C_0)$, the Heaviside step function, is 1 for $C > C_0$ and 0 for $C < C_0$. In the absence of leakage, the resting concentration would be zero. Note that a constant leakage rate, β , can always be absorbed by defining the concentration field relative to the resting level, β/Γ .

The number of independent parameters can be reduced by the introduction of dimensionless variables. The choice of the dimensional units is not unique, and is justified *a posteriori* if they give the correct scales for the quantities of interest. We present in Table 1 a set of notations that include both the dimensional (in capital letters) and dimensionless (in lowercase) parameters. We will measure the Ca²⁺ concentration in units of C_0 , time in units of C_0/J_0 , and length in units of $(C_0 D/J_0)^{1/2}$.

For uniformly propagating fronts, the concentration profile is stationary in a frame of reference moving at the pulse speed, v , i.e., it is a function of $(\tilde{x} - vt)$, where v is expressed in units of $(J_0 D/C_0)^{1/2}$. In the comoving frame of reference, $x = \tilde{x} - vt$, the profile satisfies the steady-state

TABLE 1 Summary of notations and units

Notation	Definition	Value	Units	Dimensionless form
D	Diffusion constant of free Ca^{2+}	200–300	$\mu\text{m}^2/\text{s}$	$d \equiv 1$
D_b	Diffusion constant of buffers	20	$\mu\text{m}^2/\text{s}$	$d_b \equiv D_b/D$
D_{eff}	Effective Ca-diffusion constant	22	$\mu\text{m}^2/\text{s}$	$d_{\text{eff}} \equiv D_{\text{eff}}/D$
J_0	Ca-current density through channels	2700	$\mu\text{M}/\text{s}$	$j_0 \equiv 1$
J_{eff}	Effective Ca-current density	27	$\mu\text{M}/\text{s}$	$j_{\text{eff}} \equiv J_{\text{eff}}/J_0$
$C, [\text{Ca}^{2+}]_{\text{free}}$	Free- Ca^{2+} concentration		μM	$c \equiv C/C_0$
C_0	Channel activation threshold	0.5	μM	$c_0 \equiv 1$
C_1	Channel inactivation threshold	0.6	μM	$c_1 \equiv C_1/C_0$
C_{max}	Ca wave peak amplitude		μM	$c_{\text{max}} \equiv C_{\text{max}}/C_0$
[CaB]	Buffer-bound-Ca concentration		μM	$b \equiv [\text{CaB}]/C_0$
$B, [\text{B}]_{\text{total}}$	Total buffer concentration		μM	
$B_{\text{eq}}(C)$	Equilibrium value of [CaB]		μM	$b_{\text{eq}}(c) \equiv B_{\text{eq}}(C)/C_0$
$\bar{\kappa}$	Effective buffer capacity	100		
K_f	Forward buffering reaction rate		$(\mu\text{M s})^{-1}$	$k_f \equiv (C_0^2/J_0)K_f$
K_b	Backward buffering reaction rate		s^{-1}	$k_b \equiv (C_0/J_0)K_b$
K	Forward buffer binding capacity, $K_f[\text{B}]_{\text{total}}$		s^{-1}	$k \equiv (C_0/J_0)K$
K_D	Dissociation constant K_f/K_b		μM	$k_D \equiv K_D/C_0$
T	Time		s	$t \equiv (J_0/C_0)T$
T_r	Time to threshold, $(J_{\text{eff}}D_{\text{eff}}/C_0)^{1/2}$		s	
T_{in}	Inactivation time	0.2	s	$t_{\text{in}} \equiv (J_0/C_0)T_{\text{in}}$
Γ	Pumping rate	12–25	s^{-1}	$\gamma \equiv (C_0/J_0)\Gamma$
X	Longitudinal coordinate		μm	$x \equiv (J_0/C_0D)^{1/2}X$
Λ_{eff}	$(C_0D_{\text{eff}}/J_{\text{eff}})^{1/2}$		μm	$\lambda_{\text{eff}} \equiv (J_0/C_0D)^{1/2}\Lambda_{\text{eff}}$
A	Channel spacing	0.3–0.5	μm	$a \equiv (J_0/C_0D)^{1/2}A$

equation, known as the piecewise-linear model (Rinzel and Keller, 1973):

$$\frac{d^2c}{dx^2} + v \frac{dc}{dx} - \gamma c + \Theta(c - 1) = 0 \quad (6)$$

where $c = C/C_0$ is the dimensionless concentration, and $\gamma = C_0\Gamma/J_0$ is the pumping coefficient expressed in dimensionless rate units.

Let $x = 0$ be the boundary between open ($x < 0$) and closed ($x > 0$) channels. At this boundary point, $c = 1$. Then the calcium wave profile, $c(x)$, is given by

$$c(x) = \begin{cases} 1/\gamma + A_1 e^{q^+ x} & x < 0 \\ A_2 e^{q^- x} & x > 0 \end{cases} \quad (7)$$

where A_1 and A_2 are constants to be determined, and

$$q^\pm = \frac{1}{2} [-v \pm (v^2 + 4\gamma)^{1/2}] \quad (8)$$

Matching conditions at the boundary, $c(0^-) = c(0^+) = 1$ and $c'(0^-) = c'(0^+)$, determine the front velocity:

$$v = \frac{1 - 2\gamma}{(1 - \gamma)^{1/2}} \quad (9)$$

The dimensionless pumping coefficient, γ , turns out to be a small number, and has hardly any effect on the dimensionless wave speed, which is approximately 1. In dimensional terms, this implies that $V \approx (J_0 D/C_0)^{1/2}$.

The width of the wavefront, that is, the characteristic length over which the concentration rises, is determined by

q^+ , the exponent with the smaller absolute value:

$$w = \frac{1}{q^+} = \frac{1}{\gamma}(1 - \gamma)^{1/2} \quad (10)$$

In dimensional units, this implies that $W \approx (J_0 D/C_0 \Gamma^2)^{1/2}$.

As will be shown below, the estimate for V is drastically altered by the presence of buffers, but is almost unaffected by channel inactivation. For fast buffers, an analogous form for V is obtained with the replacements $J_0 \rightarrow J_{\text{eff}}$ and $D \rightarrow D_{\text{eff}}$. On the other hand, the form of Eq. 10 for the wave width does not hold when channel inactivation is taken into account.

The effect of calcium buffering

In actual physiological systems, cytosolic calcium is strongly buffered by endogenous buffers; free Ca^{2+} ions typically constitute only 1% of the total calcium in the cytosol. Generally speaking, these buffers are poorly mobile, and they reduce both the amount of free calcium and its ability to diffuse. This directly affects wave propagation.

Let B denote a free buffer site, and let CaB denote a buffer-bound Ca^{2+} ion. The reaction can be written as



where K_f and K_b are the forward and backward reaction rates, respectively. If $[\text{B}]_{\text{total}}$ is the total buffer concentration, then *under chemical equilibrium* the bound calcium concentration, [CaB], relates to the free Ca^{2+} concentration

by the function B_{eq} :

$$[\text{CaB}] = B_{\text{eq}}([\text{Ca}^{2+}]_{\text{free}}) \equiv \frac{[\text{Ca}^{2+}]_{\text{free}}[\text{B}]_{\text{total}}}{K_{\text{D}} + [\text{Ca}^{2+}]_{\text{free}}} \quad (12)$$

where $K_{\text{D}} = K_{\text{b}}/K_{\text{f}}$ is the dissociation constant, or affinity.

Experimentally, one frequently measures the differential buffer capacity κ , that is, the total amount of calcium needed to augment $[\text{Ca}^{2+}]_{\text{free}}$ by one unit:

$$\begin{aligned} \kappa([\text{Ca}^{2+}]_{\text{free}}) &= \frac{\partial[\text{Ca}]_{\text{total}}}{\partial[\text{Ca}^{2+}]_{\text{free}}} = 1 + \frac{\partial B_{\text{eq}}}{\partial[\text{Ca}^{2+}]_{\text{free}}} \\ &= 1 + \frac{K_{\text{D}}[\text{B}]_{\text{total}}}{(K_{\text{D}} + [\text{Ca}^{2+}]_{\text{free}})^2} \end{aligned} \quad (13)$$

To account for the presence of buffers, Eq. 5 has to be replaced by a set of two equations describing the free and the bound calcium concentrations. In the comoving frame:

$$\begin{aligned} D \frac{d^2 C}{dX^2} + V \frac{dC}{dX} - \Gamma C - K_{\text{f}}([\text{B}]_{\text{total}} - [\text{CaB}])C + K_{\text{b}}[\text{CaB}] \\ + J_0 \Theta(C - C_0) = 0 \end{aligned} \quad (14)$$

$$\begin{aligned} D_{\text{b}} \frac{d^2[\text{CaB}]}{dX^2} + V \frac{d[\text{CaB}]}{dX} + K_{\text{f}}([\text{B}]_{\text{total}} - [\text{CaB}])C \\ - K_{\text{b}}[\text{CaB}] = 0 \end{aligned} \quad (15)$$

where D_{b} is the diffusion constant of buffered calcium. In dimensionless form,

$$\frac{d^2 c}{dx^2} + v \frac{dc}{dx} - \gamma c - k \left[c - c \frac{b}{b_{\text{eq}}(c)} \right] + \Theta(c - 1) = 0 \quad (16)$$

and

$$d_{\text{b}} \frac{d^2 b}{dx^2} + v \frac{db}{dx} + k \left[c - c \frac{b}{b_{\text{eq}}(c)} \right] = 0 \quad (17)$$

where the dimensionless buffer-bound calcium concentration is $b = [\text{CaB}]/C_0$ and has the equilibrium value

$$b_{\text{eq}}(c) = \frac{B_{\text{eq}}}{C_0} = \frac{[\text{B}]_{\text{total}}}{C_0} \frac{c}{k_{\text{D}} + c} = c \left(1 + \frac{c}{k_{\text{D}}} \right) [\kappa(c) - 1] \quad (18)$$

$k_{\text{D}} = K_{\text{D}}/C_0$ is the dimensionless dissociation constant, $d_{\text{b}} = D_{\text{b}}/D$ is the ratio of the buffered to free calcium diffusion constants, and $k = C_0 K_{\text{f}} [\text{B}]_{\text{total}} / J_0$ is the (maximum) forward buffer binding rate measured in units of the channel characteristic rate, J_0/C_0 .

Equations 16 and 17 are nonlinear, and there is little hope of finding an exact solution. It is, however, possible to derive simple formulas in various limiting cases, and thus to gain an understanding of the general case. In this section, we present the results. The detailed calculations are given in the Appendix.

We start by considering the linearized case. The assumption of linearity applies if the buffer is not saturated, i.e., if $c \ll k_{\text{D}}$. The buffer capacity then reduces to $\kappa \approx \kappa_0 = 1 + [\text{B}]_{\text{total}}/K_{\text{D}}$, and the bound calcium equilibrium concentration to $b_{\text{eq}}(c) = (\kappa_0 - 1)c$.

For infinitely fast reaction rates ($k \rightarrow \infty$), the linearized equations are solvable, and the wave speed is

$$v_{\infty}^{(0)}(\gamma, d_{\text{b}}) = (j_{\text{eff}} d_{\text{eff}})^{1/2} \frac{1 - 2\gamma}{(1 - \gamma)^{1/2}} \quad (19)$$

where

$$j_{\text{eff}} = \frac{1}{\kappa_0} \quad \text{and} \quad d_{\text{eff}} = \frac{1 + d_{\text{b}}(\kappa_0 - 1)}{\kappa_0} \quad (20)$$

In the expansion for speed v , order $(1/k)^i$ terms in the series expansion are denoted by the superscript (i) . An expansion about infinitely fast buffer rates is denoted by the subscript ∞ , and similarly, the expansion about infinitely slow buffering rates is denoted by the subscript 0.

Converting back to dimensional units,

$$V_{\infty}^{(0)} = \left(\frac{J_{\text{eff}} D_{\text{eff}}}{C_0} \right)^{1/2} \frac{1 - 2\gamma}{(1 - \gamma)^{1/2}} \quad (21)$$

where

$$J_{\text{eff}} = \frac{J_0}{\kappa_0} \quad \text{and} \quad D_{\text{eff}} = \frac{D + D_{\text{b}}(\kappa_0 - 1)}{\kappa_0} \quad (22)$$

Therefore, instantaneous buffering just renormalizes the diffusion constant and the rate of Ca^{2+} release. The effective diffusion constant D_{eff} is an average of the diffusion rates for free and bound calcium, weighted by their relative equilibrium concentrations. The effective Ca^{2+} release rate J_{eff} is the unbuffered flux multiplied by the fraction $1/\kappa_0$ of total calcium that is free at equilibrium. The pumping strength, Γ , which can be viewed as a negative source, is renormalized by the same factor as J_0 , and so the dimensionless parameter γ is not changed by the presence of buffers.

Next we account for fast but finite buffer reaction rates. We start by considering a system in which buffers are immobile ($d_{\text{b}} = 0$). In this case, asymptotic expansions can be derived in both limits of fast and slow buffer kinetics. For fast buffer kinetics, $k \gg 1$, the wave speed is given by the series

$$v = v_{\infty}^{(0)}(\gamma, 0) + v_{\infty}^{(1)}(\gamma, 0)k^{-1} + O(k^{-2}) \quad (23)$$

where the first two coefficients of the expansion are related by

$$\frac{v_{\infty}^{(1)}(\gamma, 0)}{v_{\infty}^{(0)}(\gamma, 0)} = [v_{\infty}^{(0)}(\gamma, 0)]^2 \frac{(\kappa_0 - 1)^2}{2} \quad (24)$$

The same quantity, written in dimensional units, is

$$\frac{V_{\infty}^{(1)}(\Gamma, 0)}{V_{\infty}^{(0)}(\Gamma, 0)} = \frac{[V_{\infty}^{(0)}(\Gamma, 0)]^2 (\kappa_0 - 1)^2}{D} \quad (25)$$

This result can be generalized for the case of mobile buffers. Rather than undertaking a lengthy calculation, we suppose that for mobile buffers one has to replace the effective diffusion constant, which for immobile buffers equals D/κ_0 , with D_{eff} . The correction factor is the ratio of these, $D/\kappa_0 D_{\text{eff}}$, or in dimensionless notation, $1/\kappa_0 d_{\text{eff}}$. Thus, for fast mobile buffers, Eqs. 23 and 24 generalize into

$$v = v_{\infty}^{(0)}(\gamma, d_b) + v_{\infty}^{(1)}(\gamma, d_b)k^{-1} + O(k^{-2}) \quad (26)$$

where

$$\frac{v_{\infty}^{(1)}(\gamma, d_b)}{v_{\infty}^{(0)}(\gamma, d_b)} = [v_{\infty}^{(0)}(\gamma, d_b)]^2 \frac{(\kappa_0 - 1)^2}{2\kappa_0 d_{\text{eff}}} \quad (27)$$

In the opposite parameter regime of slow buffer kinetics, $k \ll 1$, and immobile buffers, the wave speed is given by

$$v \approx v_0^{(0)}(\gamma, 0) + v_0^{(1)}(\gamma, 0)k + O(k^2) \quad (28)$$

where

$$v_0^{(0)}(\gamma, 0) = \frac{1 - 2\gamma}{(1 - \gamma)^{1/2}} \quad \text{and} \quad v_0^{(1)}(\gamma, 0) = -\frac{3 - 2\gamma}{2(1 - \gamma)^{3/2}} \quad (29)$$

The first term, $v_0^{(0)}(\gamma, 0)$, reduces, as expected, to the result for an unbuffered system.

Note that none of the terms in Eqs. 28 and 29 depend on the equilibrium buffer capacity, κ_0 . The physical interpretation of this is that for a slow buffer, only forward binding to buffer (k) determines the buffer's effect on wave propagation, and then only as a first-order correction. Because only the capture of calcium by buffer affects wave propagation, we also expect buffer diffusion to have little effect in the slow buffer case. In support of this, numerical calculations show that Eqs. 28 and 29 hold also for mobile buffers.

Fig. 2 shows the velocity versus the forward buffer binding capacity for $\gamma = 0.05$, $\kappa_0 = 101$, and $d_b = 0.1$. The dotted line was calculated by solving the linearized version of Eqs. 16 and 17 numerically (Eqs. 58 and 59 in the Appendix). The asymptotic approximations (*solid lines*) are very accurate, except for the intermediate range of $0.25 \leq k \leq 0.8$. For convenience, an analytical interpolation curve in this range may also be obtained (Bender and Orszag, 1978) by the use of a Padé approximant (not shown); this approximation agrees well with the numerical solution. Arrows indicate wave propagation speeds for buffers with on rates equal to those of 1,2-bis(2-aminophenoxy)ethane-*N,N,N,N*-tetraacetic acid (BAPTA) ($k = 2$) and EGTA ($k = 0.02$). For these parameter values the buffer will only slow the wave if it has a fast, BAPTA-like on rate.

We turn now to the case of buffer saturation, when buffer capacity is a nonlinear function of calcium concentration. To focus on the nonlinear aspects, we assume that the

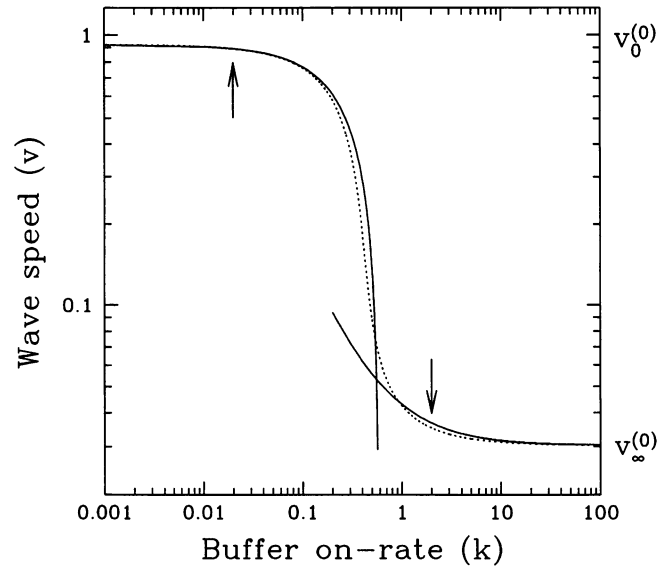


FIGURE 2 Wave speed as a function of buffer on rate. Both are plotted in dimensionless units. The dotted line is the exact solution obtained by numerically solving Eqs. 54 and 55. The solid lines are the two limiting approximations for fast and slow buffer kinetics. The parameters are $\gamma = 0.05$, $\kappa_0 = 101$, and $d_b = 0.1$. With the assumptions in the text, these are in dimensional units $\Gamma_{\text{eff}} = 2.5 \text{ s}^{-1}$ and $D_b = 30 \mu\text{m}^2/\text{s}$, and the range of on rates shown is $5\text{--}5 \times 10^5 \text{ s}^{-1}$. The arrows indicate values corresponding to $100 \mu\text{M}$ of a buffer with the on rate of BAPTA ($10^8 \text{ M}^{-1}\text{s}^{-1}$, right) or EGTA ($10^6 \text{ M}^{-1}\text{s}^{-1}$, left).

buffers are immobile and infinitely fast. Starting from Eqs. 16 and 17, the concentration profile, $c(x)$, can be shown to satisfy the equation

$$\frac{d^2c}{dx^2} + \kappa(c)v \frac{dc}{dx} - \gamma c + \Theta(c - 1) = 0 \quad (30)$$

An exact solution is not possible because of the nonlinearity of the second term. A numerical approach has been taken by Wagner and Keizer (1994).

However, an approximate solution to Eq. 30 can be obtained by the following argument. It was already pointed out that the wave speed is determined essentially at the leading edge of the channel activation front. Therefore, it ought to be possible to replace the nonlinear prefactor, $\kappa(c)$, by an appropriate average, $\bar{\kappa}$, over the region of interest. A reasonable approximation is to substitute for $\kappa(c)$ its value $\bar{\kappa}$ at a concentration, \bar{c} , near the channel activation threshold, $c = 1$. Two possible substitutions for $\bar{\kappa}$ were tested: the differential buffer capacity, $\kappa(\bar{c})$, and the overall total-to-free calcium concentration ratio, which is a different quantity when the buffer is saturable.

Comparison with numerical solutions of Eqs. 16 and 17 showed that the substitution of the total-to-free calcium concentration ratio, that is, $\bar{\kappa} = 1 + b_{\text{eq}}(\bar{c})/\bar{c}$, is a good approximation. Given this definition, it was furthermore found empirically that the best fit was obtained using $\bar{c} = 2$.

Such averaging might be generalized to also include buffer diffusion and finite reaction rates. The straightforward

ward generalization is to make the same substitution $\bar{\kappa}$ for κ_0 in Eqs. 26 and 27 (for fast buffer kinetics). We tested this conjecture by examining numerical solutions of Eqs. 16 and 17. The comparison is plotted in Fig. 3 for $\gamma = 0.05$, $[B]_{\text{total}} = 100C_0$, $k = 2, 10$, and k_D spanning the entire relevant range, between 0.1 and 5. The agreement of this approximation (*curves*) with the exact solution (*symbols*) is remarkable. This leads us to conclude that linearizing Eq. 30 by substituting $\bar{\kappa} = \kappa(2)$ in place of $\kappa(c)$ gives accurate results for wave propagation in a saturating buffer.

In the subsequent sections, in which we treat the effects of channel discreteness and inactivation, we will consider the buffers to be unsaturated. Although we do not solve for the more general case of buffer saturation, it is not unreasonable to assume that the results are likewise generalizable by the substitution $\kappa_0 \rightarrow \bar{\kappa}$.

The effect of channel discreteness

We next consider whether the discreteness of the calcium channels has a significant effect on wave propagation. To do that, we replace the continuously distributed Ca^{2+} source model by the discrete model depicted in Fig. 1. In this model the channels are uniformly spaced in one dimension with spacing A between adjacent channels. In dimensionless units, $a = A/\Lambda$, where the length scale is $\Lambda = (C_0 D/J_0)^{1/2}$.

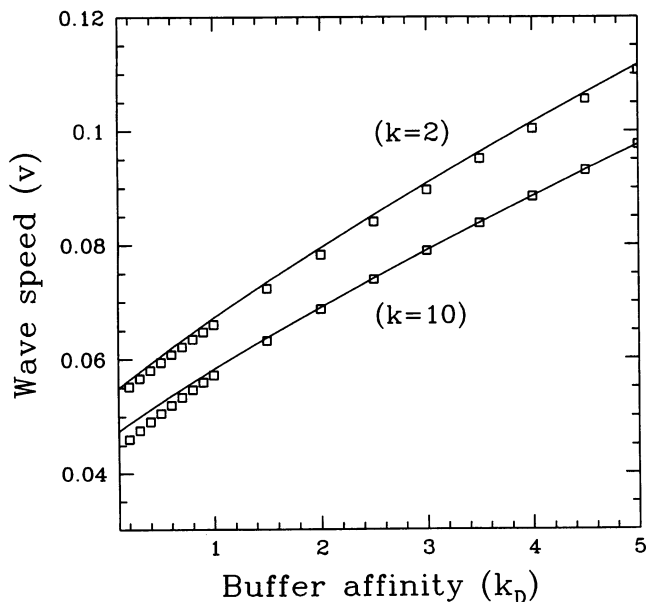


FIGURE 3 Wave speed in the presence of a saturable buffer. Wave speed v is plotted in dimensionless units (unbuffered wave speed is $v = 1$). The horizontal axis gives the buffer dissociation constant k_D in dimensionless units from 0.1 to 5; for the assumptions made in the text the dimensional axis range is 0.05–2.5 μM . The symbols are the exact numerical solution for $k = 2$ ($k_F = 0.5 \times 10^8 \text{ M}^{-1}\text{s}^{-1}$) and $k = 10$ ($k_F = 2.5 \times 10^8 \text{ M}^{-1}\text{s}^{-1}$). The solid curves are the large- k approximations with κ replaced by the total-to-free calcium ratio $\bar{\kappa}(c = 2)$. Dimensionless parameter values are $\gamma = 0.05$, $d_b = 0.1$, and $[B]_{\text{total}} = 100 C_0$. These correspond to 50 μM of a buffer with mobility $D_b = 30 \mu\text{m}^2/\text{s}$ and a pump rate of $\Gamma_{\text{eff}} = 2.5 \text{ s}^{-1}$.

To match the continuum limit, the flow through each segment of length A is then concentrated in the channel, a point source of strength $J = J_0 A$ (and in dimensionless units, $j = a$).

Buffers are assumed to be in an equilibrium binding ratio of 1:($\kappa_0 - 1$) between free and bound calcium, to be unsaturated, and have a forward buffer binding rate k . The front propagates from left to right by means of successive activation and opening of the channels. Channels open regularly at time intervals, τ , when the concentration attains the threshold value $c = 1$. We set the channel at $x = 0$ to open at time $t = 0$. The channels located at $x = -an$ opened at times $t = -n\tau$, whereas the channels at $x = am$ will open at times $t = n\tau$. Under these definitions, the front velocity is $v = a/\tau$. The mathematical details that lead to the following results can be found in the Appendix.

In the limit of infinitely fast buffer kinetics and small channel spacing, we obtain the asymptotic expansion

$$v = v_{\infty}^{(0)}(\gamma, d_b)[1 - v_{3/2}(\gamma)a_{\text{eff}}^{3/2} + v_2(\gamma)a_{\text{eff}}^2 - v_{5/2}(\gamma)a_{\text{eff}}^{5/2}] + O(a_{\text{eff}}^3), \quad (31)$$

where $a_{\text{eff}} = a/\lambda_{\text{eff}}$ and $\lambda_{\text{eff}} = (d_{\text{eff}}/j_{\text{eff}})^{1/2}$. Thus, with discretely spaced channels, the second term reduces v by a fraction that is proportional to the 3/2 power of channel spacing A on the effective length scale, $\Lambda_{\text{eff}} = (C_0 D_{\text{eff}}/J_{\text{eff}})^{1/2}$. The coefficient functions are given by

$$v_{3/2}(\gamma) = \frac{(2/\pi)^{1/2}}{12(1-\gamma)^{3/2}(1-\gamma)^{3/4}} \quad (32)$$

$$v_2(\gamma) = \frac{1}{32(1-\gamma)(1-2\gamma)} \quad (33)$$

and

$$v_{5/2}(\gamma) = \frac{(2/\pi)^{1/2}(3 - 16\gamma + 16\gamma^2)}{240(1-2\gamma)^{7/2}(1-\gamma)^{3/4}}$$

The above asymptotic expansion in Eq. 31 has the same form in both limits of fast and slow buffer kinetics. The differences are: 1) The velocity scales differ by a factor of $v_{\infty}^{(0)}/v_0^{(0)}$, and 2) The channel spacing is scaled in units of Λ_{eff} for fast buffers, rather than Λ for slow buffers. Because Λ_{eff} is longer in a buffered system than Λ for an unbuffered system, this second point implies that the continuum model is more accurate when fast buffers are present.

The effect of discreteness is less dramatic than was previously suggested by Wang and Thompson (1995). Fig. 4 shows the wave speed versus the channel spacing for a buffered system in which $\gamma = 0.01$ and $d_b = 0$ over a wide range of a . A channel spacing as large as $5\Lambda_{\text{eff}}$ ($a_{\text{eff}} = 5$) reduces the front velocity by only 20% from the continuum case. The asymptotic formula Eq. 31 gives an adequate correction up to a channel spacing of $A \approx 10\Lambda_{\text{eff}}$ ($a_{\text{eff}} \approx 10$).

This analysis assumed point sources in one dimension, which are equivalent to a series of parallel plane sources in three dimensions. For accuracy, punctate sources in a three-dimensional lattice might be more appropriate. However,

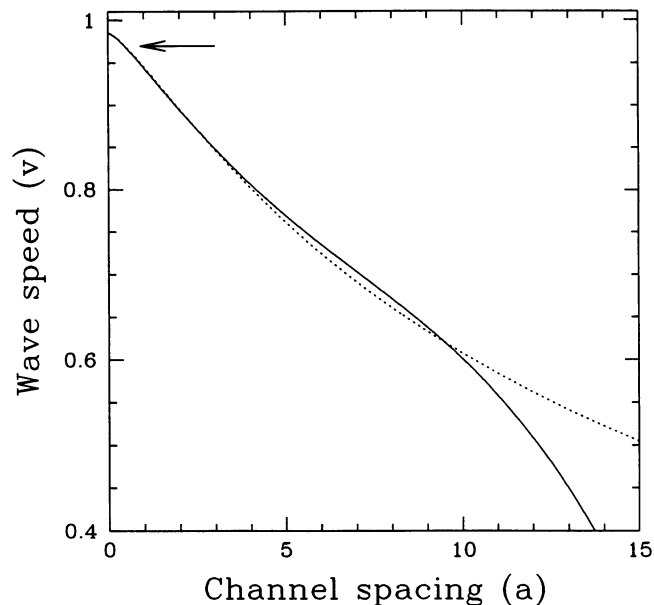


FIGURE 4 Wave speed as a function of channel spacing. Wave speed is plotted as a function of the dimensionless channel spacing a , holding fixed the amount of calcium release per unit distance. The dotted curve shows the exact numerical solution, and the solid curve shows the small- a asymptotic expression. The arrow denotes the channel spacing calculated in the text, $a_{\text{eff}} = 0.8$ ($A = 0.4 \mu\text{m}$). Parameter values are $\gamma = 0.01$ and $d_b = 0$, with an infinitely fast buffer.

our analysis would still apply to this case, because for such a diffusion-limited process the difference is only a numerical correction factor of order one.

The effect of channel inactivation

It has been assumed so far that once activated, a channel remains so indefinitely. However, an important characteristic of the IP_3 receptor is inactivation, which causes release to end and allows the restoration of a low calcium concentration.

To realistically capture this characteristic, a model of the IP_3 receptor must include both inactivation and recovery from inactivation. Unfortunately, information about these processes is incomplete. Experiments so far have focused on inactivation, which takes place in 0.025–0.2 s (Finch and Goldin, 1993; Parker et al., 1996) and is at the fast end of this range at higher Ca^{2+} concentrations (Finch and Goldin, 1993). In the steady state, activation and inactivation combine to give a probability of channel opening that is a bell-shaped curve (Bezprozvanny et al., 1991). Compared to inactivation, recovery from inactivation can be very slow. Reconstituted single channels from cerebellum take tens of seconds or longer to recover from an inactivating exposure to Ca^{2+} (E. Kaftan, personal communication), and in paired-pulse experiments in oocytes using caged IP_3 , calcium responses are depressed for seconds (Ilyin and Parker, 1994).

In previous considerations of calcium waves and oscillations, the degree of channel inactivation has been represented as a variable that we write here as $p(x, t)$. At $p = 0$ all channels are available for opening, and at $p = 1$ they are fully inactivated. The dynamics of p are coupled to calcium concentration; the form of this relationship is quite generally taken to be

$$\frac{\partial c}{\partial t} = \frac{\partial^2 c}{\partial x^2} - \gamma c + f(c)(1 - p) \quad (34)$$

$$t_{\text{in}} \frac{\partial p}{\partial t} = -p + g(c) \quad (35)$$

where $f(c)$ and $g(c)$ are rates of Ca-dependent activation and inactivation of the IP_3 receptor. In this formulation inactivation and recovery are taken to have the same characteristic time, t_{in} .

However, this approach may not be adequate because of the large difference between inactivation and recovery rates. We have chosen to concentrate on the advancing wavefront, for which recovery is not relevant. To obtain a simple model, we take the slowness of the recovery to its extreme by assuming that after inactivation, channels do not recover at all.

We assume that the Ca dependence of inactivation, $g(c)$, is a step function: inactivation is switched on when calcium rises above a threshold $c_1 = C_1/C_0$. We make a second simplification: after calcium rises above this threshold, calcium release ends not gradually, but abruptly after time T_{in} (in dimensionless units, $t_{\text{in}} = (J_0/C_0)T_{\text{in}}$). As in previous sections, the activation curve $f(c)$ is a step function $\Theta(c - 1)$. In this section we will again take buffer kinetics to be infinitely fast. As explained previously, the net effect of fast buffering is to renormalize D , J_0 , and Γ .

This model can be formulated as a single equation for the calcium concentration:

$$\frac{\partial c}{\partial t} = \frac{\partial^2 c}{\partial x^2} - \gamma c + \Theta(c - 1)\Theta[(c_1 - c(x, t - t_{\text{in}}))] \quad (36)$$

This equation is nonlocal in time (the second step function introduces a retarded process), but is still piecewise-linear and thus tractable by simple analysis. The net result is that the time-shifted inactivation $\Theta[(c_1 - c(x, t - t_{\text{in}}))]$ adds a region to the concentration profile in which channels are inactivated (Fig. 5).

For $x > 0$, the concentration is below the activation threshold, $c \leq 1$, and the channels are closed. For $-l < x < 0$, where l is a length to be determined by the calculation, the channels are activated, and the Ca^{2+} concentration rises in time. For $x < -l$, the channels are inactivated, and the concentration consequently decays, driven by pumping activity.

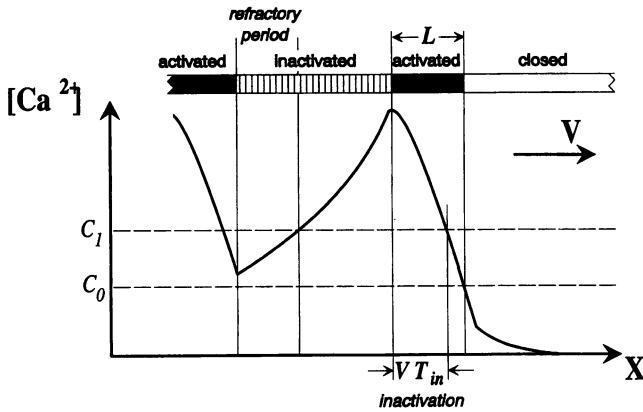


FIGURE 5 Repetitive calcium waves in a model with IP₃ receptor inactivation. In the graph calcium waves propagate with speed V in the positive x direction. The channels are at first closed (*open bar, right*) and then open (*solid bar, center*) when the Ca^{2+} concentration rises above the activation threshold C_0 . When Ca^{2+} rises above the inactivation threshold C_1 , the channels inactivate after a time delay T_{in} . For biological parameter ranges, the front length W is limited by inactivation and is approximately VT_{in} . The point $x = -W$ shows the peak of the wave and marks the boundary between activated and inactivated channels. For oscillations to occur, recovery from inactivation (*dotted bar, center*) must occur slowly enough for Ca^{2+} to be pumped below C_1 . The channels can then be reactivated (*solid bar, left*) and a second wave can be generated.

The steady-state profile has the form

$$c(x) = \begin{cases} A_1 e^{q^+ x} & x < -l \\ \frac{1}{\gamma} + A_2 e^{q^+ x} + A_3 e^{q^- x} & -l < x < 0 \\ A_4 e^{q^- x} & x > 0 \end{cases} \quad (37)$$

where

$$q^\pm = \frac{\kappa_0}{2\lambda_{eff}^2} \left[-v \pm \left(v^2 + \frac{4\gamma\lambda_{eff}^2}{\kappa_0^2} \right)^{1/2} \right] \quad (38)$$

There are five matching conditions: 1) $c(0^+) = 1$; 2) $c(0^-) = 1$; 3) $c'(0^+) = c'(0^-)$; 4) $c(-l^+) = c(-l^-)$; and 5) $c'(-l^+) = c'(-l^-)$. An additional constraint follows from the time delay of inactivation: the inactivation taking place at $x = -l$ signifies that the calcium level at this point reached c_1 at time t_{in} earlier. In the moving frame, this translates into a spatial constraint, 6) $c(t_{in}v - l) = c_1$.

The six constraints yield a set of two equations for the unknowns v and l ,

$$1 - \gamma c_1 + \frac{q^-}{q^+ - q^-} e^{q^+ v t_{in}} e^{-q^+ l} + \left(\gamma - \frac{q^+}{q^+ - q^-} \right) e^{q^- t_{in}} e^{-q^- l} = 0 \quad (39)$$

and

$$q^- l = \log[1 - \gamma(1 - q^-/q^+)] \quad (40)$$

Substituting in for q^\pm , Eq. 40 becomes

$$v = (j_{eff} d_{eff})^{1/2} \frac{1 - 2\gamma - e^{q^- l}}{(1 - \gamma - e^{q^- l})^{1/2}} \quad (41)$$

Channel activity measurements (Finch and Goldin, 1993) indicate that the two critical thresholds are very close to each other, i.e., $c_1 \approx 1$, and so $l \approx vt_{in}$. Therefore, for $t_{in} \gg 1$, as is typically the case, inactivation introduces only an exponentially small correction in the front velocity compared with Eq. 19.

On the other hand, inactivation strongly affects the concentration profile. The amplitude of the wave (at $x = -vt_{in}$) is given in the small- γ and large- t_{in} limits by

$$c_{max} \approx \frac{1}{\gamma} [1 - \exp(-\kappa_0^{-1} \gamma t_{in})] \quad (42)$$

The parameter $\kappa_0^{-1} \gamma t_{in}$ (in dimensional terms, $\Gamma_{eff} T_{in}$) determines whether the length of the rising front is dominated by pumps or by inactivation. Pump-dominated profiles are obtained when $\kappa_0^{-1} \gamma t_{in} \gg 1$. The wave amplitude in this case is approximately $1/\gamma$ (in dimensional units, J_0/Γ), and the length of the rising front is given by Eq. 10.

Inactivation-dominated profiles occur for $\kappa_0^{-1} \gamma t_{in} \ll 1$. The wave amplitude is then $c_{max} \approx j_{eff} t_{in}$, and the rising front length is $w \approx l \approx vt_{in}$. In dimensional units,

$$C_{max} \approx J_{eff} T_{in} \quad W \approx VT_{in} \quad (43)$$

A comment on calcium oscillations

Calcium oscillations are observed in a variety of cells (Prentki et al., 1988; Berridge, 1990). The two-variable model of Eqs. 34 and 35, which considers inactivation and recovery from inactivation to be symmetrical, can likewise produce sustained, constant-amplitude oscillations (cf. Atri et al., 1993). However, according to the considerations below, these oscillations occur only under conditions that are biologically implausible. This appears to be generally true for models that assume that inactivation and recovery proceed at equal rates.

In the two-variable system of Eqs. 34 and 35, oscillations are centered around fixed points, $c = c^*$ and $p = p^*$, for which $dc/dt = dp/dt = 0$. For the oscillations to be sustained, the fixed point must be unstable, so that Ca transients are not attracted to it. This condition is met when the real part of the fixed point's characteristic frequencies is positive.

Analysis of Eqs. 34 and 35 shows that satisfying this condition requires

$$\frac{1}{\gamma} \approx t_{in} \frac{f'(c^*)}{f(c^*)} \quad (44)$$

Note that this is a relationship between pump time and the intrinsic properties of the IP₃ receptor. $f'(c^*)/f(c^*)$ is the slope of the Ca activation curve divided by the total activation at concentration c^* . Inspection of measured curves

(Finch et al., 1991) reveals that $f'(c^*)/f(c^*) < 1$ at all Ca concentrations, consistent with a two-site model for activation. As a result, Ca^{2+} oscillations require that $\Gamma_{\text{eff}}T_{\text{in}} > 1$. In other words, pumping must be faster than inactivation, and wavefronts must be pump-dominated.

However, experimental observations of Γ_{eff} and T_{in} suggest that wavefronts are inactivation-dominated. The largest plausible value for this quantity in neuronal cells is $\Gamma_{\text{eff}}T_{\text{in}} = (0.25 \text{ s}^{-1})(0.2 \text{ s}) = 0.05$, much too small to support oscillations. In oocytes, a typical range for this quantity is $\Gamma_{\text{eff}}T_{\text{in}} = (1.4 \text{ s}^{-1})(0.025 - 0.125 \text{ s}) = 0.03 - 0.17$ (see Figures 1 and 5 in Parker et al., 1996). In contrast, at least one numerical model has this quantity as about 1.3 (Atri et al., 1993, assuming a peak Ca of $3 \mu\text{M}$). Although this produces oscillations, such high pump rates are inconsistent with the experimental observations.

The failure of the two-variable model to produce Ca oscillations by using biologically accurate parameters suggests that it lacks a crucial component. One possibility is suggested by the relation between rates in Eq. 44: for oscillations to occur after a wave peak, pumping must outstrip the return of IP_3 receptors from inactivation. This could be accomplished in a model by specifying that channels return slowly from inactivation, or by setting an absolute refractory period during which inactivated IP_3 receptors cannot release Ca^{2+} at all. Then only the rising phase of the wave would be dominated by inactivation, and Ca^{2+} could return to a low value before release begins again (Fig. 5). This scenario remains to be substantiated, but it is at least not a priori inconsistent with observed periods on the order of several seconds.

COMPARISON TO EXPERIMENTS

We compare our results to measurements of calcium waves in mouse neuroblastoma cells (Wang and Thompson, 1995), by calculating parameter values and computing wave parameters, and then comparing these values to experimental results.

Parameter values

Based on an average IP_3 binding site density of $5.5 \mu\text{m}^{-3}$, an average channel spacing of $0.3\text{--}0.5 \mu\text{m}$ is obtained (Wang and Thompson, 1995), depending on whether one or four IP_3 -binding sites are assumed per channel. The single-channel current through IP_3 receptor channels has been estimated to be 0.5 pA (Bezprozvanny et al., 1991). But even under optimal concentrations of IP_3 and Ca^{2+} , the open probability is only about 0.2, giving an estimated average current of 0.1 pA . The maximum release rate is then approximately $J_0 \approx 2700 \mu\text{M/s}$.

The Ca^{2+} thresholds for activation and inactivation of the IP_3 receptor were estimated from kinetic biochemical measurements of calcium release (Finch et al., 1991; Finch and Goldin, 1993). The rate of calcium release was measured as

a function of calcium concentration, immediately after a step change in Ca^{2+} , and in the steady state, after all transients were over. We used the first measurement to infer the activation characteristics. We used the second measurement to estimate inactivation characteristics, by normalizing the steady-state calcium release rate relative to its value immediately after the step change.

The activation range, defined as the concentration range of free Ca^{2+} for which the current is between 20% and 80% of its maximum value, lies between $0.15 \mu\text{M}$ and $1.4 \mu\text{M}$. Similarly, the inactivation range lies between $0.3 \mu\text{M}$ and $2.4 \mu\text{M}$. Because the Ca^{2+} dependence of these processes is graded, we used as thresholds the concentrations of calcium at which these processes are half-maximum. This gives $C_0 \approx 0.5 \mu\text{M}$ for the activation threshold, and $C_1 \approx 0.6 \mu\text{M}$ for the inactivation threshold.

Interpretation of the experimental data is complicated by overlap between the time course and Ca^{2+} dependence of activation and inactivation, and by the limited time resolution of the data (fastest sampling rate of 17 ms). These limitations cause inactivation to partially mask activation, and the activation threshold may be even higher than inferred.

Despite the fact that inactivation may occur at lower concentrations than activation, calcium excitability can still occur because activation occurs more quickly. The activation time is faster than the sampling rate and is therefore less than 17 ms . The inactivation time, on the other hand, was found to be slower, $\sim 0.1\text{--}0.2 \text{ s}$ (Finch and Goldin, 1993; E.A. Finch and J. Sneyd, personal communication).

Using the above unbuffered estimates for J_0 and C_0 , the time to reach threshold is

$$\frac{C_0}{J_0} = 0.2 \text{ ms} \quad (45)$$

and the characteristic channel rate is $J_0/C_0 = 5 \times 10^3 \text{ s}^{-1}$. Using this as the time scale and taking $T_{\text{in}} = 0.2 \text{ s}$, the dimensionless IP_3 receptor inactivation time is $t_{\text{in}} = 10^3$.

Experiments show that free Ca^{2+} is removed from the cytosol within $4\text{--}8 \text{ s}$ (Tse et al., 1994; Wang and Thompson, unpublished observations), giving $\Gamma_{\text{eff}} = 0.12\text{--}0.25 \text{ s}^{-1}$. This rate is affected by the presence of fast endogenous buffers, which typically bind 99% of the cytosolic calcium. Because only free Ca^{2+} ions are available to be pumped, the bare pumping rate in the absence of buffers is therefore higher by a factor of 10^2 , and $\Gamma = 12\text{--}25 \text{ s}^{-1}$. The corresponding dimensionless pumping rate is

$$\gamma = 2.4\text{--}5.0 \times 10^{-3} \quad (46)$$

The concentration of endogenous buffers in the cytosol has been estimated to be $[\text{B}]_{\text{total}} \approx 100 \mu\text{M}$ (Wang and Thompson, 1995), and the equilibrium total-to-free Ca^{2+} ratio is $\bar{\kappa} = 100$. This would make $J_{\text{eff}} \approx 27 \mu\text{M/s}$, consistent with the observation of Ca^{2+} release rates in oocytes of $10\text{--}150 \mu\text{M/s}$ (Parker et al., 1996). The buffer reaction on rate is closer to that of BAPTA than that of EGTA (Neher

and Augustine, 1992), and we take it to be $K_f = 10^8$ ($M s$)⁻¹. This corresponds to a dimensionless forward buffer binding capacity of $k = 2$. The diffusion constants of free and bound calcium are approximately $D = 200\text{--}300 \mu\text{m}^2 \text{s}^{-1}$ and $D_b = 20 \mu\text{m}^2 \text{s}^{-1}$. This latter number was chosen to reflect experimental conditions in which both the nearly immobile endogenous buffers (Allbritton et al., 1992; Neher and Augustine, 1992) and the mobile indicator dye, fura-2 (Baylor and Hollingworth, 1988), are present.

The effective parameters are, consequently, $D_{\text{eff}} = 22 \mu\text{m}^2 \text{s}^{-1}$ and $J_{\text{eff}}/C_0 = 50 \text{s}^{-1}$. The characteristic length scale associated with the wave is then $\Lambda_{\text{eff}} \equiv (C_0 D_{\text{eff}}/J_{\text{eff}})^{1/2} = 0.5 \mu\text{m}$, resulting in a dimensionless channel spacing of $a_{\text{eff}} = 0.8$. For this spacing, wave speed is not significantly altered from the continuum case (Fig. 4).

Note the continual distinction between “bare” and “effective” parameters. It is important in the present context; in a given calculation, one must use either the bare or the effective parameters, not a mixture of the two.

Comparison to experiments

Combining the various parameters, we obtain the following estimate for the wave speed. To leading order, the velocity is given by the basic formula for $V_{\infty}^{(0)}$. The correction due to finite buffer kinetics may be inferred from Fig. 2. For $k = 2$, the velocity is $\sim 5\%$ larger than its value in the case of infinitely fast buffer kinetics ($k = \infty$). In addition, we expect discreteness to reduce the wave speed by, at most, 2%. The effects of pumping and inactivation on the wave speed are negligible. As a result,

$$V = 1.05 \times 0.98 \left(\frac{J_{\text{eff}} D_{\text{eff}}}{C_0} \right)^{1/2} = 35 \mu\text{m/s} \quad (47)$$

This estimate matches the range of $V = 43 \pm 28 \mu\text{m s}^{-1}$ (mean \pm SD) measured by Wang and Thompson.

Note that in the present case, the corrections to $V_{\infty}^{(0)}$ are small. However, a moderate change in the buffer kinetic parameters, as can be expected among systems and even from cell to cell, will in general lead to a significant effect on wave characteristics. For example, reducing k from 2 to 1 would lead to a 30% increase in the wave speed. In fact, variation in k and in the density of IP₃-bound receptors (and therefore J_0) could easily account for the observed distribution of wave speeds.

This strong dependence of wave speed on buffering suggests that adding exogenous buffers will reduce the wave speed. In principle, the inclusion of various types of buffers requires a separate analysis, because of the existence of new time scales. Two cases are nevertheless easily treated.

In the first case, two buffers have the same mobility D_b , and the same on rate K_f . Then, one can simply define an effective buffer capacity, given by

$$\frac{1}{\kappa_{\text{eff}} - 1} = \frac{1}{\kappa_1 - 1} + \frac{1}{\kappa_2 - 1} \quad (48)$$

where κ_1 and κ_2 are the individual buffer capacities.

This case corresponds to the experiment of adding BAPTA-type chelators, the on rates of which are on the order of those of the fast endogenous buffers. The amount of added buffer was estimated through an “attenuation factor” (Wang and Thompson, 1995; see Neher and Augustine, 1992), which is roughly the ratio of the buffer capacity before (κ_1) and after (κ_{eff}) the loading of the exogenous buffers.

Equation 20 predicts that wave speed should be reduced approximately by the factor $(\kappa_{\text{eff}}/\kappa_1)^{1/2}$. Averaged over all buffers tested, the wave speed was found to decrease by 27% (Wang and Thompson, 1995). Such a decrease in the velocity would result from a doubling in the effective buffer capacity, an estimate that seems reasonable.

Because a number of different buffers of the BAPTA family were tested, it was possible to test the prediction by matching the changes in wave speed to the amount of change in buffer capacity. The comparison is complicated by the fact that the attenuation factor measures the differential buffer capacity, whereas it is the integral capacity that was found to be important in the determination of the wave speed. For buffers with low K_D , this distinction is significant, and we corrected for this.

The comparison between the measurement and the prediction is shown in Table 2. A good agreement was obtained for the 5,5'-Br₂-BAPTA/AM buffer. This buffer has a relatively large dissociation constant K_D . For 5,5'-dimethyl-BAPTA/AM, which has a small K_D , the prediction is within the experimental error bar. For the case of fura-2/AM, the difference between measurement and prediction is large. The reason for this discrepancy is unknown. It could be accounted for if fura-2 were more mobile than the other buffers and therefore less able to slow down the wave.

TABLE 2 Comparison between measured and predicted change in wave speed as a result of adding various types of fast and slow exogenous buffers

Chelator	K_D (nM)	Attenuation factor	Change in v (measurement)	Change in v (prediction)
5,5'-Dimethyl-BAPTA/AM	150	0.20 ± 0.04	$-31 \pm 22\%$	-55%
Fura-2/AM	170	0.35 ± 0.04	$-16 \pm 8\%$	-41%
5,5'-Br ₂ -BAPTA/AM	1570	0.69 ± 0.03	$-21 \pm 13\%$	-17%
EGTA/AM (slow buffer)	70	0.16 ± 0.03	$+4 \pm 12\%$	-1%

Data from Wang and Thompson (1995).

However, because the experimental error bars are large, a more accurate quantitative test of the theory awaits further experiments.

The second case applies to the experiment of adding EGTA, the on rate of which is much slower than that of the endogenous buffer. When the two on rates are very distinct, the fast ones can be accounted for first, thus obtaining renormalized parameters. The slow ones can then be treated as perturbations. The amount of added EGTA was estimated in the same way as BAPTA-type chelators.

The on rate of EGTA is about 10^6 (M s)^{-1} , which corresponds to $k = O(10^{-2})$. For such low buffering rates, the velocity is approximated by

$$V = \left(\frac{J_{\text{eff}} D_{\text{eff}}}{C_0} \right)^{1/2} \left(1 - \frac{3}{2} k \right) \quad (49)$$

where the effective parameters, J_{eff} and D_{eff} , refer to the effect of the fast endogenous buffers. Hence EGTA is expected to slow down the wave by about 1%, which matches the observed result to within experimental error (Table 2).

Next we turn to evaluate the pulse amplitude and width. Because $c_1 \approx 1$, we can use Eq. 38. The product $\bar{\kappa}^{-1} \gamma t_{\text{in}}$ determines whether the pulse shape is dominated by inactivation or by the pumps. For the above data, we find that $\bar{\kappa}^{-1} \gamma t_{\text{in}} = 0.04$. Hence the pulse shape will be mainly determined by inactivation, with height

$$C_{\text{max}} = 5.4 \text{ } \mu\text{M} \quad (50)$$

The wave amplitude as estimated from the experiments is typically below $3 \text{ } \mu\text{M}$. The discrepancy may lie partly in the fact that dyes commonly used for Ca^{2+} detection saturate at these high concentrations. The width of the rising front is given by

$$W = VT_{\text{in}} = 7 \text{ } \mu\text{m} \quad (51)$$

The wave width was measured to be $W = 13.3 \pm 5.5 \text{ } \mu\text{m}$ (mean \pm SD), which matches this calculation.

DISCUSSION

The analysis presented in this paper provides simple relations between the main calcium wave characteristics and the underlying microscopic parameters. These calculations apply to systems in which the positive feedback necessary to sustain wave propagation is provided by calcium-induced calcium-release (CICR) at the IP_3R . The propagation speed is then determined by a combination of the effective calcium diffusion constant D_{eff} , and the time scale of the feedback loop, which is inversely proportional to the effective release rate J_{eff} .

Here “effective” refers to the values of quantities as modified by buffers, in contrast to “bare” or unbuffered quantities. For example, the release rate in the absence of buffers J_0 is replaced by an effective value $J_{\text{eff}} = J_0/\bar{\kappa}$, where $\bar{\kappa}$ is the buffer capacity. Because $\bar{\kappa}$ is large in cells,

buffers therefore have a significant impact on effective properties.

The effects of buffers are describable entirely in terms of parameter renormalization only if the buffers are infinitely fast. Finite kinetics introduce subleading corrections, which depend on the ratio of the binding reaction rate and the rate of the CICR feedback loop. These corrections are generally significant. For linear, or nonsaturated buffers, we obtained analytical formulas for the limits of fast and slow buffer kinetics.

The influence of buffers increases with buffer concentration, but this effect is suppressed by buffer saturation. For saturable buffers, these analytical formulas are still reasonably accurate, provided that the Ca^{2+} -dependent buffer capacity is replaced by an appropriate average value. The concentration profile of a wave, whether the cell responds by a single wave or generates a repetitive train, is divided into two qualitatively distinct regions: a rising front followed by a decaying tail. The length of the rising front is governed by the receptor inactivation time T_{in} . This is the duration of calcium release, and it therefore determines both the pulse amplitude and the rising front length. During the decaying part, a low-calcium state must be restored before the receptors may be activated again, and this is therefore governed by pumping activity.

All of the corrections that we have considered may be summarized by the following cumulated expression for wavefront velocity:

$$V = \left(\frac{J_{\text{eff}} D_{\text{eff}}}{C_0} \right)^{1/2} \left\{ 1 - \frac{3}{2} \frac{\Gamma}{J_0/C_0} + \frac{1}{2} \frac{J_0/C_0}{K_f[\text{B}]_{\text{total}}} - \frac{(2/\pi)^{1/2}}{12} \left[\frac{A}{(C_0 D_{\text{eff}}/J_{\text{eff}})^{1/2}} \right]^{3/2} - \frac{3}{2} \exp\left(-\frac{T_{\text{in}}}{C_0/J_0}\right) \right\} \quad (52)$$

The variable terms within the curly brackets are, respectively, first-order corrections arising from pumping, fast buffers, channel discreteness, and channel inactivation. The numerical coefficients to these corrections (i.e., $(2/\pi)^{1/2}/12$) are model dependent. However, the parameter groupings are model independent and reveal the appropriate scales for these biological phenomena when considering calcium wave generation.

Our analytical result for wave speed parallels earlier theories. The expression for the speed of a wave propagated by an autocatalytic reaction together with diffusion, $V \sim (D_{\text{eff}}/T_r)^{1/2}$, goes back to Luther (Luther, 1906; Jaffe, 1991), where T_r is a characteristic time for calcium rise to close the feedback loop. For the particular case of propagation by calcium-induced calcium release, our calculation for $V_{\infty}^{(0)}$ is made equivalent to this expression by taking $T_r = J_{\text{eff}}/C_0$.

An alternative theory for Ca wave propagation was proposed by Meyer (1991). Meyer proposed a simple expression for the rising front length, $W = (DT_r)^{1/2}$. Combined with Luther's equation, it gives the relation $W \cdot V = D$. Sneyd and Kalachev have pointed out that this expression is wrong because buffering is not taken into account, and they

propose a relation for systems with infinitely fast buffers (Sneyd and Kalachev, 1994; Sneyd et al., 1995). Here we have shown that another problem with Meyer's expression is that it does not take channel inactivation into account. All of these relations rely on the assumption that the CICR feedback time scale T_r is equal to the total duration of calcium release, which is in general not true. The duration of calcium release is in fact longer and is limited by the inactivation time.

To summarize, the correct expressions are

$$V \approx \left(\frac{D_{\text{eff}}}{T_r} \right)^{1/2} \quad (53)$$

$$W \approx \left(\frac{D_{\text{eff}}}{T_r} \right)^{1/2} T_{\text{in}} \quad (54)$$

$$W \cdot V \approx \left(\frac{T_{\text{in}}}{T_r} \right) D_{\text{eff}} \quad (55)$$

The length-speed product, $W \cdot V$, has been measured by Wang and Thompson (1995). Their interpretation of this quantity, in terms of previous theory, as a diffusion constant is not correct, for the reasons we have discussed. The correct interpretation is that the length-speed product expresses a relationship between calcium diffusion and IP_3R flux, activation, and inactivation parameters. Given our assumption for D_{eff} , the observation by Wang and Thompson that $W \cdot V \approx 400 \mu\text{m}^2/\text{s}$ then implies that the positive feedback loop is about 20 times faster than IP_3 receptor inactivation, a conclusion well in agreement with observed properties of the IP_3 receptor.

Our analysis of calcium wave propagation has correctly predicted a number of experimental results: fundamental wave parameters, and the slowing of waves by fast buffers but not slow ones. However, the strength of our approach remains to be more rigorously tested both experimentally and theoretically.

A central future experimental test is the full exploration of the effects of buffer loading on waves. We have predicted that when fast buffers are added to the cytoplasm, wave speed will be inversely proportional to the square root of the total buffer strength; results so far confirm this prediction. However, more detailed quantitative measurements are needed, not only of wave slowing by buffers, but of all the fundamental parameters—calcium pumping, IP_3 metabolism, and IP_3 receptor density and kinetics—in a single biological preparation. This has not yet been done.

We note two outstanding theoretical problems that remain: how waves are initiated, and why receptor stimulation leads to a single wave in some cells, and to an oscillatory sequence of waves in others.

One key to understanding wave initiation is the observation that calcium release is delayed by several seconds after cell stimulation (Prentki et al., 1988; Wang et al., 1995). Because during this delay period IP_3 concentration may still be rising toward a plateau, it is possible that the delay is

caused by the time required for IP_3 to reach a threshold concentration that supports initiation and propagation of a calcium wave (Wang et al., 1995).

This IP_3 threshold can be explained within the framework of our discrete model. When IP_3 is low, the effective channel spacing is increased and the effective current density decreased. The question is then whether there exists a threshold density of channels below which waves cannot propagate. An absolute minimum criterion is that at large channel spacing, release must continue for a long enough time to activate the neighboring channels before channel inactivation takes place. Under this constraint, the fraction of IP_3 -bound receptors p must satisfy the inequality

$$\frac{C_0}{pJ_{\text{eff}}} < T_{\text{in}} \quad (56)$$

For the parameter values we have used, this gives a minimum value for p of 0.1. This corresponds to either 10% saturation of receptors, or to complete saturation of IP_3R spaced at an average distance of 0.7–1.0 μm . The delay to calcium wave initiation would then be explained by a rise in IP_3 until activated receptors are closer than this critical distance. Then spontaneous opening of a channel would be the trigger for Ca^{2+} release. This mechanism could explain the strongly nonlinear nature of the IP_3 dose-response relationship (Parker and Ivorra, 1993; Parker et al., 1996).

The characterization of repetitive wave trains, and notably the condition that determines whether a cell generates a single pulse or a periodic wave, is beyond the scope of this paper. Here we have shown that even establishing such conditions for a uniformly oscillating cell requires a better understanding of how channels and stores recover from inactivation.

Periodic wave phenomena add a theoretical challenge: these wave characteristics do not simply follow from the microscopic parameters by dimensional arguments. In repetitive waves, the nonlinearity of the activation and inactivation curves plays a subtle role. Typically, reaction-diffusion equations for an excitable medium do not even determine a unique wave frequency, but rather give rise to a continuous family of allowed solutions (Rinzel and Keller, 1973). A full explanation of these complex phenomena will require experimental resolution of and theoretical accounting for detailed biological mechanisms.

APPENDIX

The effect of unsaturated buffers

For unsaturated buffers, the buffer capacity is constant, and equals the total-to-free calcium concentration ratio:

$$\kappa_0 = 1 + \frac{b_{\text{eq}}(c)}{c} \quad (57)$$

Equations 16 and 17 reduce, then, to the piecewise-linear form,

$$\frac{d^2c}{dx^2} + v \frac{dc}{dx} - \gamma c - k \left(c - \frac{b}{\kappa_0 - 1} \right) + \Theta(c - 1) = 0 \quad (58)$$

and

$$d_b \frac{d^2b}{dx^2} + v \frac{db}{dx} + k \left(c - \frac{b}{\kappa_0 - 1} \right) = 0 \quad (59)$$

The large- k limit is treated by expanding $b(x)$ in $1/k$ about its equilibrium value,

$$b(x) = (\kappa_0 - 1)c(x) + \eta(x)k^{-1} + O(k^{-2}) \quad (60)$$

which, substituted into Eq. 59, gives to leading order

$$(\kappa_0 - 1)\eta(x) = d_b(\kappa_0 - 1)c''(x) + v(\kappa_0 - 1)c'(x) \quad (61)$$

Substituting this back into Eq. 58, we obtain a single equation for the free Ca^{2+} concentration,

$$\lambda_{\text{eff}}^2 \frac{d^2c}{dx^2} + \kappa_0 v \frac{dc}{dx} - \gamma c + \Theta(c - 1) = 0 \quad (62)$$

where $\lambda_{\text{eff}}^2 = 1 + d_b(\kappa_0 - 1)$. Equation 62 is completely analogous to Eq. 6 up to different coefficients, which can be adjusted by resealing the coordinates. The resulting velocity is given by Eq. 19.

The finite- k cases can be solved for immobile buffers ($d_b = 0$). The general solution of Eqs. 58 and 59 is

$$c(x) = \begin{cases} \frac{1}{\gamma} + A_1 e^{q_1 x} + A_2 e^{q_2 x} & x < 0 \\ A_3 e^{q_3 x} & x > 0 \end{cases} \quad (63)$$

and

$$b(x) = \begin{cases} \frac{\kappa_0 - 1}{\gamma} + B_1 e^{q_1 x} + B_2 e^{q_2 x} & x < 0 \\ B_3 e^{q_3 x} & x > 0 \end{cases} \quad (64)$$

where $q_{1,2,3}$ are, respectively, the two positive roots and the one negative roots of the cubic equation,

$$v q^3 + \left(v^2 - \frac{k}{\kappa_0 - 1} \right) q^2 - v \left(\frac{\kappa_0 k}{\kappa_0 - 1} + \gamma \right) q + \frac{\gamma k}{\kappa_0 - 1} = 0 \quad (65)$$

There are now four matching conditions at $x = 0$, the additional one being $c''(0^+) - c''(0^-) = 1$. By straightforward manipulations, one finally obtains the following implicit equation for the front velocity:

$$q_3^2 \left(2q_3 v + v^2 - \frac{k}{\kappa_0 - 1} \right) + \frac{1 - \gamma}{\kappa_0 - 1} k - q_3 v = 0 \quad (66)$$

The asymptotic expansions for $k \ll 1$ and $k \gg 1$ are obtained by expanding q and v in powers of k and k^{-1} , respectively, substituting into Eqs. 65 and 66, and equating term by term.

The effect of channel discreteness

Let $G_c(x, t)$ denote the concentration of $[\text{Ca}^{2+}]_{\text{free}}$ at point x and time t contributed from a channel placed at the origin and that opened at time $t = 0$. $G_b(x, t)$ is the corresponding bound calcium concentration. Both satisfy

the set of equations

$$\frac{\partial G_c}{\partial t} = \frac{\partial^2 G_c}{\partial x^2} - \gamma G_c - k \left(G_c - \frac{G_b}{\kappa_0 - 1} \right) + a \delta(x) \Theta(t) \quad (67)$$

$$\frac{\partial G_b}{\partial t} = d_b \frac{\partial^2 G_b}{\partial x^2} + k \left(G_c - \frac{G_b}{\kappa_0 - 1} \right) \quad (68)$$

The solution can be found in momentum space using the Fourier-cosine transform,

$$G_c(x, t) = \frac{2}{\pi} \int_0^\infty dq \cos(qx) G_c(q, t) \quad (69)$$

with a similar definition for $G_b(q, t)$. The solution for $G_c(q, t)$ reads

$$G_c(q, t) = \frac{a}{2r(q)} + \frac{a}{2[s^+(q) - s^-(q)]} \left[\left(1 + \frac{s^-(q)}{r(q)} \right) e^{s^+(q)t} - \left(1 + \frac{s^+(q)}{r(q)} \right) e^{s^-(q)t} \right] \quad (70)$$

where $s^\pm(q)$ are the two roots of the quadratic equation

$$s^2 + \left[(1 + d_b)q^2 + \gamma + \frac{\kappa_0 k}{\kappa_0 - 1} \right] s + \frac{\lambda_{\text{eff}}^2 q^2 + \gamma}{\kappa_0 - 1} k + d_b q^2 (q^2 + \gamma) = 0 \quad (71)$$

and

$$r(q) = \left[1 + \frac{d_b(\kappa_0 - 1)}{1 + d_b(\kappa_0 - 1)q^2 k^{-1}} \right] q^2 + \gamma \quad (72)$$

As there are an infinite number of open channels along the negative x axis, the concentration at the origin is the sum over functions $G_c(x, t)$, due to sources located at distances na away, and which opened in the past at times $t = -n\tau = -na/v$, with $n = 1, 2, \dots$. Then the condition that the concentration at the origin at time $t = 0$ equals the activation threshold,

$$c(0, 0) = \sum_{n=1}^\infty G_c(x = na, t = n\tau) = 1, \quad (73)$$

determines the wave speed as a function of γ , k , κ_0 , and a .

The problem is significantly simplified in the limit of fast buffer kinetics. To leading order, $s^-(q) = -\kappa_0 k / (\kappa_0 - 1)$ and $s^+(q) = -(\lambda_{\text{eff}}^2 q^2 + \gamma) / \kappa_0$. In this case, Eq. 70 reduces to

$$G_c(q, t) = \frac{a}{2(\lambda_{\text{eff}}^2 q^2 + \gamma)} \left\{ 1 - \exp \left[-\frac{\lambda_{\text{eff}}^2 q^2 + \gamma}{\kappa_0} t \right] \right\} \quad (74)$$

for which the inverse transform is

$$G_c(x, t) = -\frac{a}{4\gamma^{1/2}\lambda_{\text{eff}}} \left[e^{\gamma^{1/2}\hat{x}} \text{erfc} \left(\frac{\hat{x}}{2\hat{t}^{1/2}} + \hat{t}^{1/2}\gamma^{1/2} \right) - e^{-\gamma^{1/2}\hat{x}} \text{erfc} \left(\frac{\hat{x}}{2\hat{t}^{1/2}} - \hat{t}^{1/2}\gamma^{1/2} \right) \right] \quad (75)$$

(Oberhettinger, 1957), where $\hat{x} = x/\lambda_{\text{eff}}$, and $\hat{t} = t/\kappa_0$.

To proceed, we have to calculate infinite series of the form

$$I = \sum_{n=1}^{\infty} e^{\rho n} \operatorname{erfc}[(\sigma a n)^{1/2}] \quad (76)$$

where ρ and σ are arbitrary parameters. For small values of a , these series can be approximated by an integral

$$\begin{aligned} I \approx \frac{1}{\sigma a} \int_{\sigma a/2}^{\infty} dx e^{(\rho/\sigma)x} \operatorname{erfc}(x^{1/2}) &\sim -\frac{1}{\rho a} + \frac{1}{\rho a} \frac{\sigma^{1/2}}{(\rho - \sigma)^{1/2}} - \frac{1}{2} \\ &+ \frac{2^{1/2}}{3\pi^{1/2}} (\sigma a)^{1/2} - \frac{1}{8} \rho a + \frac{2^{1/2}}{30\pi^{1/2}} (3\rho - \sigma) \sigma^{1/2} a^{3/2} \\ &+ O(a^2) \end{aligned} \quad (77)$$

Substitution of Eq. 75 into Eq. 73, and use of the asymptotic expansion 77, gives for the front velocity

$$\begin{aligned} v \approx v_{\infty}^{(0)}(\gamma, d_b) \left[1 - \frac{(2/\pi)^{1/2} a_{\text{eff}}^{3/2}}{12(1-2\gamma)^{3/2}(1-\gamma)^{3/4}} \right. \\ \left. + \frac{a_{\text{eff}}^2}{32(1-\gamma)(1-2\gamma)} \right. \\ \left. - \frac{(2/\pi)^{1/2}(3-16\gamma+16\gamma^2)a_{\text{eff}}^{5/2}}{240(1-2\gamma)^{7/2}(1-\gamma)^{3/4}} \right] + O(a_{\text{eff}}^3) \end{aligned} \quad (78)$$

with $a_{\text{eff}} = a/\lambda_{\text{eff}}$.

RK thanks David Kessler for helpful advice. Beth Finch, Ed Kaftan, and James Sneyd made results available before publication, and an anonymous reviewer made a number of valuable comments.

Noted added in proof: E. Oancea and T. Meyer (1996) have directly measured recovery from IP₃ receptor inactivation and found that its time course in RBL cells roughly matches the interval between Ca spikes, in consistency with our prediction (*J. Biol. Chem.* 271:17253–17260).

REFERENCES

- Allbritton, N. L., T. Meyer, and L. Stryer. 1992. Range of messenger action of calcium ion and inositol 1,4,5-trisphosphate. *Science*. 258:1812–1814.
- Atri, A., J. Amundson, D. Clapham, and J. Sneyd. 1993. A single-pool model for intracellular calcium oscillations and waves in the *Xenopus laevis* oocyte. *Biophys. J.* 65:1727–1739.
- Baker, P. F., and A. C. Crawford. 1972. Mobility and transport of magnesium in squid giant axons. *J. Physiol. (Lond.)* 227:855–874.
- Baylor, S. M., and S. Hollingworth. 1988. Fura-2 calcium transients in frog skeletal muscle fibers. *J. Physiol. (Lond.)* 403:151–192.
- Bender, M., and S. A. Orszag. 1978. *Advanced Mathematical Methods for Scientists and Engineers*. McGraw-Hill, New York.
- Berridge, M. J. 1990. Calcium oscillations. *J. Biol. Chem.* 265:9583–9586.
- Berridge, M. J. 1993. Inositol trisphosphate and calcium signaling. *Nature*. 361:315–325.
- Bezprozvanny, I., J. Watras, and B. E. Ehrlich. 1991. Bell-shaped calcium-response curves of Ins(1,4,5)P₃ and calcium-gated channels from endoplasmic reticulum of cerebellum. *Nature*. 351:751–754.
- De Young, G. W., and J. Keizer. 1992. A single-pool inositol 1,4,5-trisphosphate-receptor-based model for agonist-stimulated oscillations in Ca²⁺ concentration. *Proc. Natl. Acad. Sci. USA*. 89:9895–9899.
- Dupont, G., and A. Goldbeter. 1994. Properties of intracellular Ca²⁺ waves generated by a model based on Ca²⁺-induced Ca²⁺ release. *Biophys. J.* 67:2191–2204.
- Finch, E. A., and S. M. Goldin. 1993. Dynamic regulation of IP₃-dependent calcium release by extravesicular calcium. *Soc. Neurosci. Abstr.* 485.20.
- Finch, E. A., T. J. Turner, and S. M. Goldin. 1991. Calcium as a coagonist of inositol 1,4,5-trisphosphate-induced calcium release. *Science*. 252:443–446.
- Gyorke, S., and M. Fill. 1993. Ryanodine receptor adaptation: control mechanism of Ca²⁺-induced Ca²⁺ release in heart. *Science*. 260:807–809.
- Herrington, J., Y. B. Park, D. F. Babcock, and B. Hille. 1996. Dominant role of mitochondria in clearance of large Ca²⁺ loads from rat adrenal chromaffin cells. *Neuron*. 16:219–228.
- Iino, M., and M. Endo. 1992. Calcium-dependent immediate feedback control of inositol 1,4,5-trisphosphate-induced Ca²⁺ release. *Nature*. 360:76–78.
- Ilyin, V., and I. Parker. 1994. Role of cytosolic Ca²⁺ in inhibition of InsP₃-evoked Ca²⁺ release in *Xenopus* oocytes. *J. Physiol. (Lond.)* 477:503–509.
- Jaffe, L. F. 1991. The path of calcium in cytosolic calcium oscillations: a unifying hypothesis. *Proc. Natl. Acad. Sci. USA*. 88:9883–9887.
- Jafri, M. S., and J. Keizer. 1995. On the role of Ca²⁺ diffusion, Ca²⁺ buffers, and the endoplasmic reticulum in IP₃-induced Ca²⁺ waves. *Biophys. J.* 69:2139–2153.
- Lechleiter, J., S. Girard, E. Peralta, and D. Clapham. 1991. Spiral wave propagation and annihilation in *Xenopus laevis* oocytes. *Science*. 253:123–126.
- Luther, R. 1906. Propagation of chemical reactions in space. *Z. Elektrochem.* 12:596.
- McKean, H. P. 1970. Nagumo's equation. *Adv. Math.* 4:209–223.
- Meyer, T. 1991. Cell signaling by second messenger waves. *Cell*. 64:675–678.
- Murray, J. D. 1989. *Mathematical Biology*. Springer-Verlag, Berlin.
- Neher, E., and G. J. Augustine. 1992. Calcium gradients and buffers in bovine chromaffin cells. *J. Physiol. (Lond.)* 450:273–301.
- Oberhettinge, F. 1957. *Tabellen zur Fourier transformation*. Springer-Verlag, Berlin.
- Parker, I., and I. Ivorra. 1993. Confocal microfluorimetry of Ca²⁺ signals evoked in *Xenopus* oocytes by photoreleased inositol trisphosphate. *J. Physiol. (Lond.)* 461:133–165.
- Parker, I., Y. Yao, and V. Ilyin. 1996. Fast kinetics of calcium liberation induced in *Xenopus* oocytes by photoreleased inositol trisphosphate. *Biophys. J.* 70:222–237.
- Prentki, M., M. C. Glennon, A. P. Thomas, R. L. Morris, F. M. Matschinsky, and B. E. Corkey. 1988. Cell-specific patterns of oscillating free Ca²⁺ in carbamylcholine-stimulated insulinoma cells. *J. Biol. Chem.* 263:11044–11047.
- Rinzel, J., and J. B. Keller. 1973. Traveling wave solutions of a nerve conduction equation. *Biophys. J.* 13:1313.
- Sneyd, J., S. Girard, and D. Clapham. 1993. Calcium wave propagation by calcium-induced calcium release: an unusual excitable system. *Bull. Math. Biol.* 55:315–344.
- Sneyd, J., and L. V. Kalachev. 1994. A profile analysis of propagating calcium waves. *Cell Calcium*. 15:289–296.
- Sneyd, J., J. Keizer, and M. J. Sanderson. 1995. Mechanisms of calcium oscillations and waves: a quantitative analysis. *FASEB J.* 9:1463–1472.
- Tang, Y., and Y. Othmer. 1994. A model of calcium dynamics in cardiac myocytes based on the kinetics of ryanodine-sensitive calcium channels. *Biophys. J.* 67:2223–2235.
- Tse, A., W. Tse, and B. Hille. 1994. Calcium homeostasis in identified rat gonadotrophs. *J. Physiol. (Lond.)* 477:511–525.
- Wagner, J., and J. Keizer. 1994. Effect of rapid buffers on Ca²⁺ diffusion and Ca²⁺ oscillations. *Biophys. J.* 67:447–456.
- Wang, S. S.-H., A. A. Alousi, and S. H. Thompson. 1995. The lifetime of inositol 1,4,5-trisphosphate in single cells. *J. Gen. Physiol.* 105:149–171.
- Wang, S. S.-H., and S. H. Thompson. 1995. Local positive feedback by calcium in the propagation of intracellular calcium waves. *Biophys. J.* 69:1683–1697.
- Winfree, A. T. 1987. *When Time Breaks Down: The Three-Dimensional Dynamics of Electrochemical Waves and Cardiac Arrhythmias*. Princeton University Press, Princeton, NJ.